metals

MDPI

Article

Unveiling the Alloying-Processing-Microstructure Correlations in High-Formability Sheet Magnesium Alloys

Jiyong Yang [1], Renhai Shi [1,2,*] and Alan A. Luo [3,4,*]

[1] Beijing Advanced Innovation Center for Materials Genome Engineering, University of Science and Technology Beijing, Beijing 100083, China
[2] Institute for Materials Intelligent Technology, Liaoning Academy of Materials, Shenyang 110004, China
[3] Department of Materials Science and Engineering, The Ohio State University, Columbus, OH 43210, USA
[4] Department of Integrated Systems Engineering, The Ohio State University, Columbus, OH 43210, USA
* Correspondence: renhai.shi.nick@gmail.com (R.S.); luo.445@osu.edu (A.A.L.)

Abstract: Designing magnesium sheet alloys for room temperature (RT) forming is a challenge due to the limited deformation modes offered by the hexagonal close-packed crystal structure of magnesium. To overcome this challenge for lightweight applications, critical understanding of alloying-processing–microstructure relationship in magnesium alloys is needed. In this work, machine learning (ML) algorithms have been used to fundamentally understand the alloying-processing–microstructure correlations for RT formability in magnesium alloys. Three databases built from 135 data collected from the literature were trained using 10 commonly used machine learning models. The accuracy of the model is obviously improved with the increase in the number of features. The ML results were analyzed using advanced SHapley Additive exPlanations (SHAP) technique, and the formability descriptors are ranked as follows: (1) microstructure: texture intensity > grain size; (2) annealing processing: time > temperature; and (3) alloying elements: Ca > Zn > Al > Mn > Gd > Ce > Y > Ag > Zr > Si > Sc > Li > Cu > Nd. Overall, the texture intensity, annealing time and alloying Ca are the most important factors which can be used as a guide for high-formability sheet magnesium alloy design.

Keywords: magnesium alloys; room temperature formability; machine learning; SHAP evaluation; alloy design

check for updates

Citation: Yang, J.; Shi, R.; Luo, A.A. Unveiling the Alloying-Processing-Microstructure Correlations in High-Formability Sheet Magnesium Alloys. *Metals* **2023**, *13*, 704. https://doi.org/10.3390/met13040704

Academic Editor: Antonio Mateo

Received: 20 February 2023
Revised: 21 March 2023
Accepted: 26 March 2023
Published: 3 April 2023

Copyright: © 2023 by the authors. Licensee MDPI, Basel, Switzerland. This article is an open access article distributed under the terms and conditions of the Creative Commons Attribution (CC BY) license (https://creativecommons.org/licenses/by/4.0/).

1. Introduction

Lightweight magnesium (Mg) and its alloys with low density and high specific strength are increasingly used for industrial applications [1,2] in automotive, aerospace, and electronic sectors. Compared to aluminum (Al) alloys [3,4] and steels [5], however, applications of commercial wrought Mg alloys are hampered due to their limited formability at room and low temperatures, caused by insufficient plastic deformation and mobility of non-basal dislocations. Over the last two decades, attempts have been made to investigate the fundamental plastic deformation mechanisms and improve the cold stretch formability via tailoring the addition of alloying elements [6–8] and thermomechanical processing (TMP) [9,10] of Mg sheet alloys. Additions of zinc (Zn), calcium (Ca), and manganese (Mn) of Mg alloys [11–14] and trace additions of rare-earth elements such as yttrium (Y), neodymium (Nd), and cerium (Ce) can significantly improve ductility or formability, which is attributed to reduce intrinsic stacking fault I1 energy (I1 SFE) [15], lower critical resolved shear stress (CRSS) of pyramidal $\langle c + a \rangle$ slip [16], and weakened strong basal texture [17]. Chino et al. [18] studied the relationship between Zn content and tensile formability of rolled Mg-xZn-0.2Ce alloy. It is found that the addition of dilute Zn with more than 0.5 wt.% effectively weakens the basal texture and makes it split towards transverse direction(TD) which improves the deformability of the alloy. When the Zn content is 1.5 wt.%, the Erichsen value of the alloy reaches 9.0, which is equivalent to that of commercial aluminum alloy. Cai et al. [19] studied the effects of Y, Ce and Gd on the texture

and tensile formability of Mg-1.5Zn alloy. It is found that the addition of Y, Ce and Gd can effectively weaken and improve the basal texture of magnesium alloy, which is helpful to improve the tensile formability. In addition, the Erichsen value of Mg-1.5Zn-0.2Sc alloy designed by Bian et al. [20] reached 8.6. The Erichsen value of Mg-1.5Zn-0.2Y alloy studied by Yasumasa Chino et al. [6] reached 9.1. A large number of research results show that rare earth elements play a significant role in improving the formability of magnesium alloys, but it is worth noting that the addition of Ca elements to magnesium alloys can also produce similar results as rare earth elements. Chino et al. [21,22] have studied the effect of small amount of Ca on the tensile formability of Mg alloy sheet at room temperature. It was found that the Erichsen values of Mg-1.5Zn-0.1Ca alloy and Mg-3Zn-0.1Ca alloy were 14.1% and 98% higher than those of Mg-1.5Zn (3.4) alloy and Mg-3Zn (4.1) alloy, respectively. Based on the analysis of its microstructure, it is considered that the improvement of the formability of the alloy is due to the decrease in the basal texture strength and the expansion to the direction of TD after adding Ca element. Thermomechanical processing (TMP) such as homogenization, rolling and annealing is also important in tailoring Mg microstructure for final mechanical properties. Homogenization, maximizing the alloying effect, has been studied via CALPHAD modeling and experimental characterization for its influence on the mechanical properties and formability of Mg-Zn-Al-Ca-Ce-Mn alloy and showed that better homogenization could attribute to better formability, due to its weak and split basal texture and fine grain structure [23]. High temperature rolling, as one alternative way, has also been demonstrated to improve the stretch formability of Mg alloy at room/low temperature. Such improvement could be ascribed to the enhancement of activity of pyramidal <c + a> slips and the weakened basal texture [24–29]. Bian et al. [9] studied the effect of different rolling conditions on the formability of Mg-1.2Al-0.3Ca-0.4Mn-0.3Zn alloy and attributed the better formability to the weak basal texture and fine grain structure formed during rolling. Huang et al. [27] studied the effect of finishing temperature on the microstructure, texture, mechanical properties and tensile formability of magnesium alloy. When the rolling temperature increases from 723 K to 798 K, the Erichsen value increases significantly from 4.5 to 8.6 due to the weakening of texture. Fukuoka et al. [30] studied the effect of rolling temperature on the formability and texture of Mg-Al-Sn (AT31) alloy sheet at room temperature. It is found that higher rolling temperature will bring better room temperature formability. In addition, the reason why the texture of AT31 alloy is smaller than that of AZ31 alloy rolled under the same conditions is that there are more randomly oriented grains recrystallized on the grain boundary during the final annealing heat treatment.

It is clear from the above that alloying and thermomechanical processing could affect the microstructure of Mg alloys such as texture and grain size. Thus, it is important to understand the contributions of various descriptors to the formability of Mg alloys at room and low temperatures. These descriptors can be categorized into alloy descriptors (alloy elements and concentration), TMP descriptors (temperature and time), and microstructural descriptors (texture and grain size). The descriptors (alloying-processing-structure) related to RT formability in multicomponent alloy systems have been mostly studied via CALPHAD (CALculation of Phase Diagrams) modeling [31–38], as a part of Integrated Computational Materials Engineering (ICME) framework [39]. However, the relationship between the descriptors and RT formability of Mg alloys is not fully understood for high-formability magnesium sheet alloy design.

As a data-driven technique, machine learning (ML) algorithms can effectively explore complex relationships between data features [40]. Large-scale R & D activities in the field of materials have accumulated a large amount of data, which lays a foundation for the wide application of machine learning methods in material research. In recent years, machine learning methods have shown good prospects, for example, in alloy phase classification and phase structure prediction, material microscopic image analysis, and material service behavior prediction. It is worth noting that machine learning is used to establish a "black box" hidden structure–activity relationship between material influencing factors (such

as composition and technology) and target quantities (such as properties, microstructure, and phase composition). It can realize the prediction of material composition, structure, process, and properties and the auxiliary design of new materials. Liu et al. [41] established an alternative model between hardness and input characteristics (composition and aging conditions). The composition and heat treatment process of Mg-Al-Sn-Zn-Ca-Mn alloy were optimized by active learning method, which effectively guided the development of high hardness cast magnesium alloy. In order to improve the strength and plasticity of as-cast ZE62 magnesium alloy, Chen et al. [42] optimized the two-step aging process parameters by using machine learning aided design strategy, and realized the multi-objective optimization of alloy design. Mi et al. [43] established the relationship between synthesis processing and target performance via optimizing the input of the artificial neural network in a reverse machine learning design model (RMLDM) with a particle swarm optimization algorithm. Wang et al. [44] successfully designed low SFE rare earth-free Mg alloys based on the correlation analysis between the atomic features (volume, first ionization energy, bulk modulus) in a ML algorithm and the SFE values calculated by density functional theory (DFT). Qiao et al. [45] have especially revealed the relationship between hardness and element descriptors in multicomponent alloys (MACs) through machine learning and first-principles calculations.

Machine learning can also help material scientists to deeply understand the mechanism characteristics of materials and understand the scientific nature of material problems from different scales and different dimensions. Gui et al. [46] successfully predicted the twin nucleation behavior of Mg alloys and disclosed the important contribution of the data features on twin nucleation of Mg alloys via ML and electron backscatter diffraction (EBSD) techniques. Messina et al. [47] used atomic simulation combined with machine learning technology to study the segregation of Alelements at grain boundaries, showing the potential of machine learning technology in the calculation of physical properties of grain boundaries. Jung et al. [48] use machine learning technology combined with a small number of full-field simulation results to construct accurate structure–property relationships in a wide range of microstructure, and achieve the use of less full-field simulation to identify microstructure with optimal characteristics.

In addition, the application of machine learning in the manufacturing processes also attracts attention. Ortego et al. [49] proposed a network hyperparameter optimization method based on evolutionary algorithm, and on this basis proposed a deep learning model for pattern classification. It shows excellent accuracy and practicability in the test scenarios involving the installation process of shutter fasteners in the aviation industry. Mirandola et al. [50] used ML algorithm to predict the energy consumption of radial axial ring rolling process. Palmieri et al. [51] used the machine learning model to optimize the forming process parameters, and put forward a method to control the blank holder force in the deep drawing process in real time. Wang et al. [52] studied the intelligent recognition model of hot rolled strip surface defects based on convolution neural network (CNN). Using defect image database, a defect recognition model based on CNN is established. The results show that high recognition accuracy can be obtained in a short time by this model. Wu et al. [53] proposed a prediction model based on multidimensional support vector regression, and combined a feature selection method involving the correlation representation of maximum information coefficients and complex network clustering to reduce the input dimension. The mechanical properties of steel are predicted according to the conditions of four main processes (smelting, continuous casting, hot rolling, and cold rolling). This method has the lowest computational complexity on the premise of high prediction accuracy.

The predictive capability of ML models strongly depends on the amount and quality of the dataset. It should be particularly addressed on the improvement of the MLs' predictive effectiveness with the limited amount of datasets in the design of Mg sheet alloy. In this paper, we focus on (1) improving ML models' predictive capability with the limited amount of dataset via cross-sectionally expanding the formability descriptors (alloying element,

concentration, processing temperature, time, grain size, and texture intensity) of each dataset in various MLs; (2) investigating the influence of various descriptors and ML algorithms on the formability of Mg sheet alloy; and (3) disclosing their important contribution to improving the stretch formability of Mg sheet alloy at room/low temperature.

2. Methods

Firstly, relevant data were collected from references and data cleaning was performed, and finally a raw dataset including alloying descriptors (metal element, nominal composition), processing descriptors (annealing temperature and time), microstructural descriptors (texture and grain size), and Erichsen values of the Mg alloys including Mg-Zn and Mg-Al base alloys with a total of 135 entries were constructed and shown in Table 1 and supplementary material (Figure S1) for more detail. It should be noted that the effect of precipitation will not be considered in datasets of this work due to the high-temperature annealing heat treatment. In addition, the rolling process of magnesium alloy sheet will also not be considered in the datasets due to lack of enough and uniform data for describing the complex deformation processing. Thus, the contribution of minor amounts of second phases and various rolling processing will be studied in the near future via coupling with the experimental design. To represent the variation in cross-sectional characteristics, three datasets were created as Dataset 1, Dataset 2 and Dataset 3 on the basis of the original dataset.

Table 1. Definitions and range of the formability descriptors in dataset.

Descriptor	Definition	Range
Compositions (wt%)	Al	0–9.07
	Zn	0–6.2
	Ca	0–2.1
	Mn	0–1.3
	Y	0–4.2
	Zr	0–0.5
	Sr	0–2
	Ag	0–11
	Ce	0–0.2
	Li	0–3
	Gd	0–2.74
	Sc	0–1.5
	Cu	0–0.31
	Nd	0–2.3
	Si	0–0.22
Annealing Process	Temperature (K)	473–753
	Time (h)	0.25–8
Microstructure	Grain size (um)	5–63
	Texture (mrd)	2–18.4
Stretch formability	Index Erichsen (mm)	1.7–10.7

Dataset 1: (Input) alloying descriptors → (Output) Erichsen Index;

Dataset 2: (Input) alloying descriptors + processing descriptors → (Output) Erichsen Index;

Dataset 3: (Input) alloying descriptors + processing descriptors + microstructural descriptors → (Output) Erichsen Index.

Secondly, 10 algorithmic models are implemented using the scikit-learn library, including Kernel ridge regression (KRR), Gaussian process regression (GPR), extreme tree regression (ETR), random forest regression (RFR), support vector machine regression (SVR), gradient boosting regression (GBR), Bagging_SVR, Bagging_KNR, XGBoost, and CatBoost.

To maximize the usefulness of the models, each dataset was normalized using the Standard Scaler module when applied to some of the models. During the modeling process, the data were randomly divided into training and test sets in a 4:1 ratio, and hyperparameter search was performed for each model using grid search with 10-fold cross-validation. In other words, the training dataset was randomly divided into 10 folds and the models are

trained on any 9 folds to obtain training accuracy and validated on the remaining 1 fold to obtain cross-validation accuracy. The validation process was then repeated 10 times until each fold was validated exactly once and the 10 training/cross-validation accuracies were averaged to produce a single estimated accuracy. The accuracy of the training and cross-validation results was evaluated by the coefficient of determination (R^2) as follows:

$$R^2 = 1 - \frac{\sum_{i=1}^{n}(y_i - \hat{y}_i)}{\sum_{i=1}^{n}(y_i - \overline{y}_i)} \tag{1}$$

where $\hat{y}$ is the model-predicted value for each solute i, y_i is the original value and $\overline{y}_i$ is the mean value of y_i. The value of R^2 ranges from 0 to 1, with 1 indicating a perfect model. It is noted that the value of R^2 of training results represents the ability of a model to fit known data, while that of cross-validation results indicates the ability to predict unknown data, that is, model generality. Overfitting occurs in a model if the former approaches 1 and is much higher than the latter. To intuitively understand the error of a model in terms of Index Erichsen value, the performances of models were additionally assessed using root-mean-square error (*RMSE*):

$$RMSE = \sqrt{\frac{1}{n}\sum_{i=1}^{n}(y_i - \hat{y}_i)^2} \tag{2}$$

The smaller the *RMSE* is, the better the model performance is. Note that *RMSE* can only be compared between models using the same dataset. Finally, the change in prediction accuracy is shown via comparing between different models with the same dataset and via comparing various datasets with the same model. To further elucidate the relationship between features and Erichsen values, SHapley Additive exPlanations (SHAP) analysis was introduced to interpret the models and rank the feature importance. The SHAP method is a new unified approach to interpret model predictions proposed by Lundberg and Lee in 2017 [54].

3. Results and Discussion

The basic flow in this work is shown in Figure 1, which consists of three main steps, i.e., establishment of datasets, construction of ML models and analysis of important contribution of formability descriptors via ML models with SHAP algorithm. The input dataset for ML algorithms generally consists of alloying composition for materials design, which usually requires a large amount of compositional datasets for improving accuracy of ML models. In this work, the accuracy of 10 ML models based on the limited amount of compositional dataset was evaluated via cross-sectionally expanding the formability descriptors including processing descriptors (annealing temperature and time) and microstructural descriptors (texture and grain size) into each compositional dataset, which can be categorized into Dataset 1, Dataset 2 and Dataset 3 shown in Figure 1. The critical contributions of formability descriptors could be calculated via the trained ML model and SHAP methods to identify the important factors on improving the stretch formability of Mg sheet alloy at room temperature, which can be used for design of Mg sheet alloy with high RT formability.

It is critical for the maximum likelihood model to establish the mapping relationship between data descriptors. More accurate descriptor relationship will lead to less error in the machine learning predictions. Figure 2 shows the heat map of Pearson's correlation coefficients between the descriptors, the linear correlation between most of descriptors is very weak, and their correlation coefficient does not exceed 0.4. In other words, there are no significant redundant features in the database used in this work. In this work, Erichsen values (I.E.) were set as the target descriptor. It can be seen that there is no obviously linear relationship between I.E. and these descriptors, which suggests that the Erichsen value of Mg alloys is determined by various factors rather than a simple monotonic or linear relationship. The main reasons for this phenomenon are the complex interactions among the alloying elements, process parameters and microstructure, which would affect the

plastic deformation mechanisms and thus stretch formability of Mg sheet alloy. Therefore, it is difficult to generalize with a simple linear relationship between target descriptor (I.E.) and other input descriptors as shown in Figure 2. Thus, a nonlinear algorithm is recommended for more accurate machine learning models in this work.

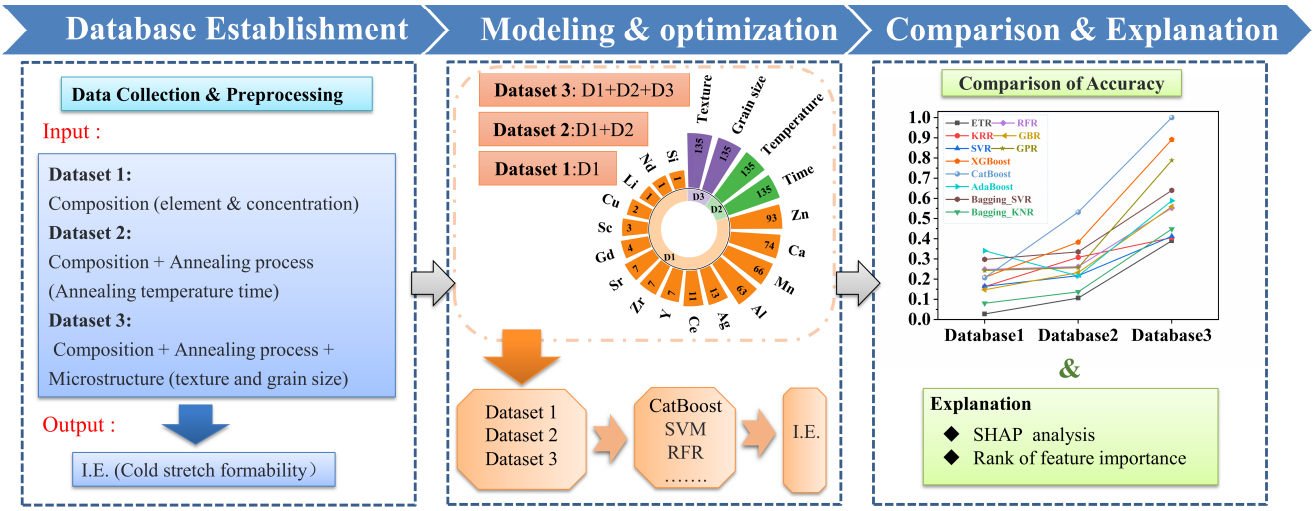

Figure 1. The detailed workflow about the important contribution of formability descriptors on cold stretch formability of Mg sheet alloy in this work via machine learning and SHAP methods.

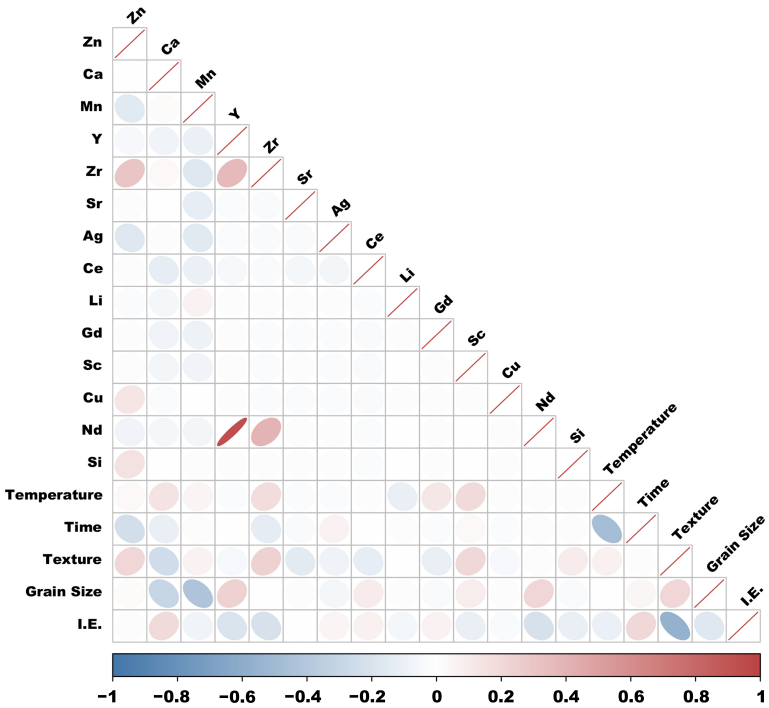

Figure 2. Correlation coefficients between all formability descriptors.

After training the 10 algorithmic models and performing hyperparameter optimization, the accuracy of the test set of 10 ML models on each dataset was calculated in Figure 3a, in which the accuracy of the training set was between 0.8 and 0.95. To highlight the gap between different ML algorithms on each dataset, the R^2 of test set of CatBoost model with the best prediction is used as the benchmark 1 to demonstrate the relative accuracy of other ML models on various datasets and the results are summarized in Figure 3a. All ML models showed an increasing accuracy via expanding the Dataset 1 to Dataset 2 with the annealing

process descriptors, in which the accuracy is increased by 287.5% for ETR model and 157% for CatBoost model. When the dataset is further expanded from Dataset 2 to Dataset 3 by adding microstructural descriptors, the accuracy of all ML models is further improved, with 267.7% accuracy enhancement for ETR model, 227.5% for Bagging_KNR model, 207.3% for GPR model, and more than 100% for the remaining models such as RFR, GBR, and XGBoost. Overall, the accuracy of all ML models based on the limited compositional dataset shows a significant improvement via cross-sectionally expanding the formability descriptors such as processing and microstructural descriptors in datasets. Figure 3b shows the influence of adding various amount of formability descriptors on the accuracy of CatBoost model. The resulting calculation shows that the root–mean–square error (RMSE) of the CatBoost model is decreased with the addition of formability descriptors, suggesting that the accuracy of CatBoost model is increased. Therefore, it can be concluded that the cross-sectional expansion of descriptors could effectively improve the accuracy of the ML models with a small dataset.

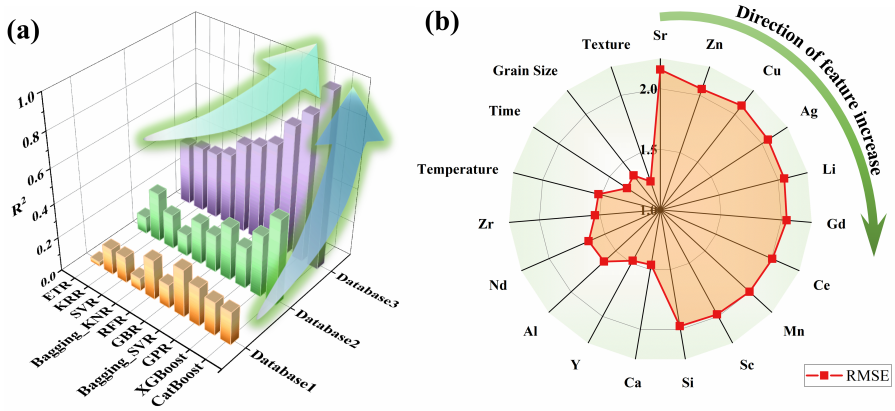

Figure 3. (**a**) Test set accuracy of different ML models on three datasets, (**b**) Variation of CatBoost model accuracy with the accumulation of descriptors.

To reveal the effect of formability descriptors on ML model accuracy, the SHAP values of each descriptor was calculated based on the CatBoost model in the SHAP library. As shown in Figure 4a, a positive/negative SHAP value of a feature (formability descriptor) means that the feature (formability descriptor) raises/lowers the value of Erichsen Index. For each feature, the data points on the horizon line have more coverage and its impact on the predicted result is greater, suggesting this feature is more important on the ML model. In Figure 4a, the calculating result suggests that the texture intensity, grain size and the content of Al has an inverse relationship with the SHAP value; however, the annealing time, the content of Ca and Zn are proportional to the SHAP value. In Figure 4b, the average of the absolute SHAP values of a feature can be considered as one factor evaluating its importance on the value of Erichsen index. It can be found that the texture intensity is the most important descriptor. In other words, texture acts as an important role affecting formability of magnesium sheet alloys, which has been verified in the most of experimental research. As also shown in Figure 4a, the texture intensity is smaller and the SHAP value is larger, which suggesting that the value of Erichsen Index is higher for better formability.

Figure 5a shows the variation of SHAP value with texture intensity. The calculation shows that the texture intensity has an inverse relationship with SHAP value, also plotted in Figure 4a. It should be particularly noted that the SHAP value is significantly increased to be positive when the texture intensity is decreased to 6 mrd, which suggests that the value of Erichsen index (I.E.) is possibly higher with the texture intensity less than 6 mrd. The experimental Erichsen index and texture intensity used in the datasets were summarized in Figure 5b with the corresponding SHAP values. In Figure 5b, the high values of Erichsen index are indeed concentrated in the range of texture intensity less than 6 mrd, which is

consistent with the calculated results in Figure 5a, and a large number of studies [18–23] have shown that the change in texture will have a significant impact on formability.

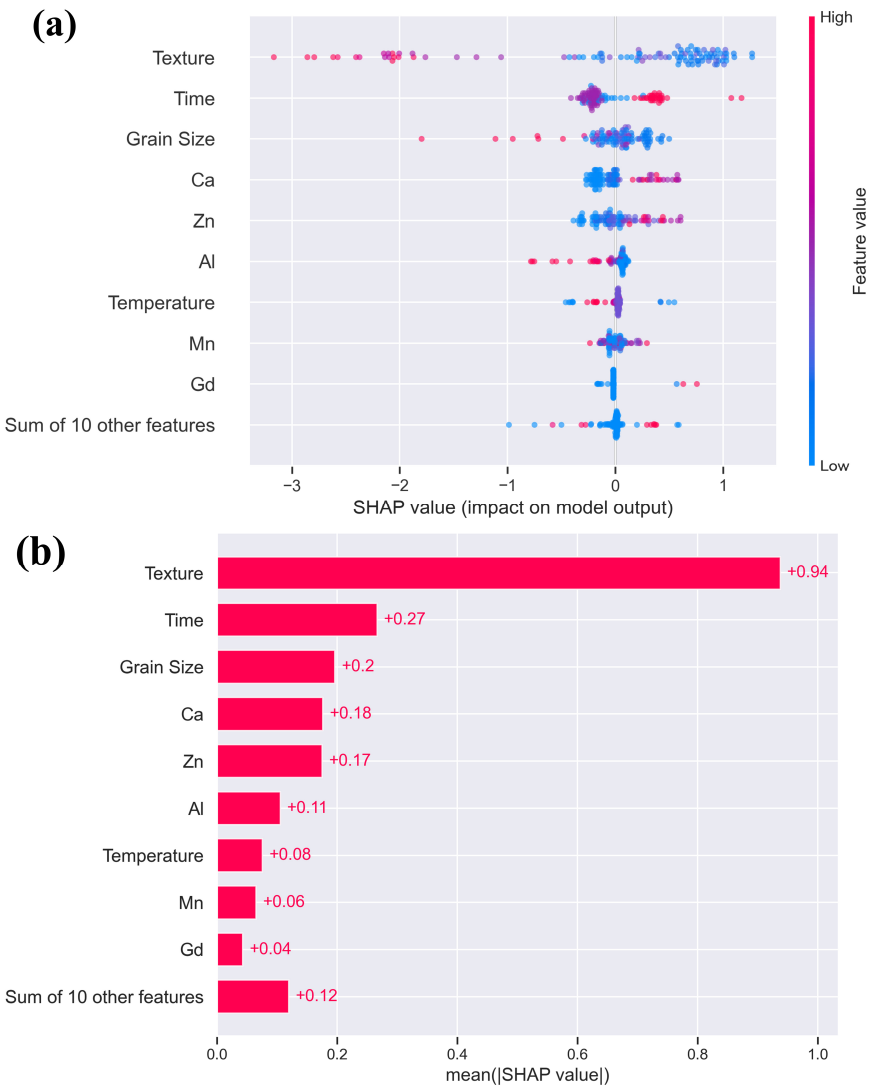

Figure 4. The feature analysis via SHAP method. (**a**) SHAP value distribution of different samples, (**b**) Feature importance ranked by SHAP value.

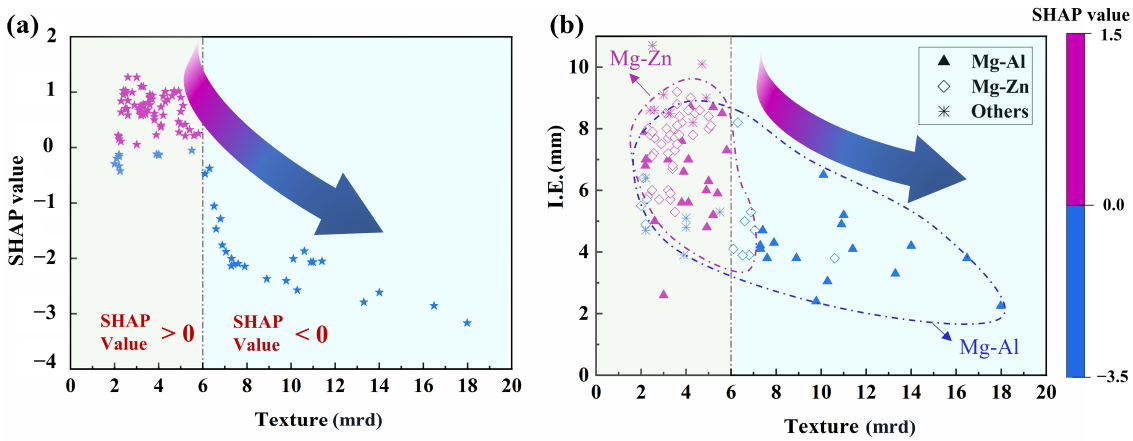

Figure 5. (**a**) The SHAP value and (**b**) I.E. change with texture intensity of Mg alloys.

Except for texture intensity, the following three important descriptors on the formability of Mg sheet alloy in Figure 4b are predicted as annealing time, grain size and Ca alloying, which are related to the annealing process, microstructure, and alloying additions. Annealing time can affect the recrystallization behavior of magnesium alloy during annealing, and has a great influence on grain size and texture [55]. There is a certain degree of negative correlation between grain size and formability, indicating that the smaller the grain size is, the better the formability is. This is consistent with the general belief that grain refinement can improve the stress distribution of materials during deformation and improve the ability of synergistic plastic deformation [56,57]. The positive effect of Ca content on formability has also been shown in Figure 4b and is known to be an alternative of rare earth elements for weakening texture. Overall, the improvement of formability of Mg sheet alloy could be attributed to lower texture intensity, longer annealing time, smaller grain size, more additions of Ca and Zn as well as less addition of Al.

The results show that there is a strong correlation between texture strength and formability on small data sets, but limited by the amount of data, it may not be able to describe this relationship very accurately. On the technical side, our findings provide a solution to the problem of "how to improve the accuracy of models built with small datasets". In terms of the understanding of the material itself, we successfully extract the key attributes for the target performance from the data by analyzing the importance of material attributes (input features) in the model. These works can speed up the progress of establishing an accurate model and show the hidden relationships in material properties from the point of view of data, which provides a new method for in-depth understanding of the internal relations of material properties. The next work will focus on improving the amount of data in the database to establish a more accurate data-driven model to better reflect this relationship and lay the foundation for further performance prediction and component-aided design.

4. Conclusions

The accuracy of ML models based on a limited amount of compositional dataset (Dataset 1) could be significantly improved via cross-sectionally expanding the formability descriptors. The SHAP analysis of the trained ML model suggests the following important contributions of each formability descriptor. (1) Microstructure: texture intensity > grain size; (2) annealing processing: time > temperature; and (3) alloying elements: Ca > Zn > Al > Mn > Gd > Ce > Y > Ag > Zr > Si > Sc > Li > Cu > Nd.

Compared to the accuracy of ML models with small amount of compositional dataset, the accuracy is improved more than 100% for all 10 ML models and more than 200% for 6 of 10 ML models with the cross-sectionally expanding formability descriptors such as processing descriptors (annealing temperature and time) and microstructural descriptors (texture and grain size).

1. Through SHAP analysis, it is found that the most important factor affecting the Erichsen value in this work is texture intensity, followed by annealing time, grain size, and Ca content in the categories of microstructure, annealing process, and alloying element, respectively, which is consistent with the previous experimental research.
2. When the texture intensity is less than 6 mrd, the value of Erichsen index is significantly increased. When the texture intensity is more than 6 mrd, the SHAP value decreases rapidly. The value of Erichsen index also shows a similar trend with SHAP value.
3. The room-temperature formability of Mg sheet alloy could be improved through lower texture intensity, longer annealing time, smaller grain size, more additions of Ca and Zn as well as less addition of Al.

Supplementary Materials: The following supporting information can be downloaded at: https://www.mdpi.com/article/10.3390/met13040704/s1, Figure S1: Data distribution of the database. References [58–88] are cited in the supplementary materials.

Author Contributions: Conceptualization, A.A.L.; Formal analysis, J.Y.; Data curation, J.Y.; Writing—original draft, J.Y.; Writing—review and editing, R.S. and A.A.L.; Supervision, R.S.; Project administration, R.S.; Funding acquisition, R.S. All authors have read and agreed to the published version of the manuscript.

Funding: J.Y. and R.S. gratefully acknowledge the support from National Key Research and Development Program of China (No. 2021YFB3700700 and No. 2021YFB3700701) and Fundamental Research Funds for the Central Universities under Award Numbers (06109209 and 06500161). AAL acknowledges the support from The Ohio State University.

Data Availability Statement: The data are available from the corresponding author on reasonable request.

Conflicts of Interest: The authors declare no conflict of interest.

References

1. Pollock, T.M. Weight Loss with Magnesium Alloys. *Science* **2010**, *328*, 986–987. [CrossRef] [PubMed]
2. Lu, K. The future of metals. *Science* **2010**, *328*, 319–320. [CrossRef] [PubMed]
3. Horita, Z.; Ohashi, K.; Fujita, T.; Kaneko, K.; Langdon, T.G. Achieving High Strength and High Ductility in Precipitation-Hardened Alloys. *Adv. Mater.* **2005**, *17*, 1599–1602. [CrossRef]
4. Zhao, Y.H.; Liao, X.; Cheng, S.; Ma, E.; Zhu, Y.T. Simultaneously Increasing the Ductility and Strength of Nanostructured Alloys. *Adv. Mater.* **2006**, *18*, 2280–2283. [CrossRef]
5. Jiang, S.; Wang, H.; Wu, Y.; Liu, X.; Chen, H.; Yao, M.; Gault, B.; Ponge, D.; Raabe, D.; Hirata, A.; et al. Ul-trastrong steel via minimal lattice misfit and high-density nanoprecipitation. *Nature* **2017**, *544*, 460–464. [CrossRef]
6. Chino, Y.; Sassa, K.; Mabuchi, M. Texture and stretch formability of a rolled Mg–Zn alloy containing dilute content of Y. *Mater. Sci. Eng. A* **2009**, *513–514*, 394–400. [CrossRef]
7. Trang, T.T.T.; Zhang, J.H.; Kim, J.H.; Zargaran, A.; Hwang, J.H.; Suh, B.-C.; Kim, N.J. Designing a magnesium alloy with high strength and high formability. *Nat. Commun.* **2018**, *9*, 2522. [CrossRef]
8. Chino, Y.; Sassa, K.; Mabuchi, M. Tensile Properties and Stretch Formability of Mg-1.5 mass%-0.2 mass%Ce Sheet Rolled at 723 K. *Mater. Trans.* **2008**, *49*, 1710–1712. [CrossRef]
9. Bian, M.Z.; Sasaki, T.T.; Nakata, T.; Kamado, S.; Hono, K. Effects of rolling conditions on the microstructure and mechanical properties in a Mg–Al–Ca–Mn–Zn alloy sheet. *Mater. Sci. Eng. A* **2018**, *730*, 147–154. [CrossRef]
10. Chino, Y.; Sassa, K.; Mabuchi, M. Texture and stretch formability of Mg-1.5 mass% Zn-0.2 mass% Ce alloy rolled at different rolling temperatures. *Mater. Trans.* **2008**, *49*, 2916–2918. [CrossRef]
11. Bian, M.Z.; Sasaki, T.T.; Suh, B.C.; Nakata, T.; Kamado, S.; Hono, K. A heat-treatable Mg–Al–Ca–Mn–Zn sheet alloy with good room temperature formability. *Scr. Mater.* **2017**, *138*, 151–155. [CrossRef]
12. Zeng, Z.R.; Zhu, Y.M.; Xu, S.W.; Bian, M.Z.; Davies, C.H.J.; Birbilis, N.; Nie, J.F. Texture evolution during static recrystallization of cold-rolled magnesium alloys. *Acta Mater.* **2016**, *105*, 479–494. [CrossRef]
13. Zhang, B.P.; Geng, L.; Huang, L.J.; Zhang, X.X.; Dong, C.C. Enhanced mechanical properties in fine-grained Mg–1.0 Zn–0.5 Ca alloys prepared by extrusion at different temperatures. *Scr. Mater.* **2010**, *63*, 1024–1027. [CrossRef]
14. Robson, J.; Henry, D.; Davis, B. Particle effects on recrystallization in magnesium–manganese alloys: Particle-stimulated nucleation. *Acta Mater.* **2009**, *57*, 2739–2747. [CrossRef]
15. Sandlöbes, S.; Friák, M.; Zaefferer, S.; Dick, A.; Yi, S.; Letzig, D.; Pei, Z.; Zhu, L.-F.; Neugebauer, J.; Raabe, D. The relation between ductility and stacking fault energies in Mg and Mg–Y alloys. *Acta Mater.* **2012**, *60*, 3011–3021. [CrossRef]
16. Liu, G.; Zhang, J.; Xi, G.; Zuo, R.; Liu, S. Designing Mg alloys with high ductility: Reducing the strength discrepancies between soft deformation modes and hard deformation modes. *Acta Mater.* **2017**, *141*, 1–9. [CrossRef]
17. Luo, A.A.; Mishra, R.K.; Sachdev, A.K. High-ductility magnesium–zinc–cerium extrusion alloys. *Scr. Mater.* **2011**, *64*, 410–413. [CrossRef]
18. Chino, Y.; Huang, X.; Suzuki, K.; Sassa, K.; Mabuchi, M. Influence of Zn Concentration on Stretch Formability at Room Temperature of Mg–Zn–Ce Alloy. *Mater. Sci. Eng. A* **2010**, *528*, 566–572. [CrossRef]
19. Cai, Z.X.; Jiang, H.T.; Tang, D.; Ma, Z.; Kang, Q. Texture and Stretch Formability of Rolled Mg–Zn–Re (Y, Ce, and Gd) Alloys at Room Temperature. *Rare Metals* **2013**, *32*, 441–447. [CrossRef]
20. Bian, M.; Huang, X.; Mabuchi, M.; Chino, Y. Compositional optimization of Mg–Zn–Sc sheet alloys for enhanced room temperature stretch formability. *J. Alloys Compd.* **2019**, *818*, 152891. [CrossRef]
21. Chino, Y.; Huang, X.; Suzuki, K.; Mabuchi, M. Enhancement of Stretch Formability at Room Temperature by Addition of Ca in Mg-Zn Alloy. *Mater. Trans.* **2010**, *51*, 818–821. [CrossRef]
22. Chino, Y.; Ueda, T.; Otomatsu, Y.; Sassa, K.; Huang, X.; Suzuki, K.; Mabuchi, M. Effects of Ca on Tensile Properties and Stretch Formability at Room Temperature in Mg-Zn and Mg-Al Alloys. *Mater. Trans.* **2011**, *52*, 1477–1482. [CrossRef]
23. Shi, R.; Miao, J.; Luo, A.A. A new magnesium sheet alloy and its multi-stage homogenization for simultaneously improved ductility and strength at room temperature. *Scr. Mater.* **2019**, *171*, 92–97. [CrossRef]

24. Huang, X.; Suzuki, K.; Saito, N. Textures and stretch formability of Mg–6Al–1Zn magnesium alloy sheets rolled at high temperatures up to 793 K. *Scr. Mater.* **2009**, *60*, 651–654. [CrossRef]
25. Huang, X.; Suzuki, K.; Saito, N. Enhancement of stretch formability of Mg–3Al–1Zn alloy sheet using hot rolling at high temperatures up to 823 K and subsequent warm rolling. *Scr. Mater.* **2009**, *61*, 445–448. [CrossRef]
26. Huang, X.; Suzuki, K.; Chino, Y.; Mabuchi, M. Improvement of stretch formability of Mg–3Al–1Zn alloy sheet by high temperature rolling at finishing pass. *J. Alloys Compd.* **2011**, *509*, 7579–7584. [CrossRef]
27. Huang, X.; Suzuki, K.; Chino, Y.; Mabuchi, M. Influence of aluminum content on the texture and sheet formability of AM series magnesium alloys. *Mater. Sci. Eng. A* **2015**, *633*, 144–153. [CrossRef]
28. Huang, X.; Suzuki, K.; Chino, Y.; Mabuchi, M. Texture and stretch formability of AZ61 and AM60 magnesium alloy sheets processed by high-temperature rolling. *J. Alloys Compd.* **2015**, *632*, 94–102. [CrossRef]
29. Bian, M.; Huang, X.; Chino, Y. Substantial improvement in cold formability of concentrated Mg–Al–Zn–Ca alloy sheets by high temperature final rolling. *Acta Mater.* **2021**, *220*, 117328. [CrossRef]
30. Fukuoka, H.; Huang, X.; Suzuki, K.; Tsukada, Y.; Koyama, T.; Chino, Y. Effect of Rolling Temperature on Room Temperature Formability and Texture Formation of Mg-3 mass%Al-1 mass%Sn Alloy Sheet. *J. Jpn. Inst. Met. Mater.* **2021**, *85*, 120–127. [CrossRef]
31. Shi, R.; Chandra, D.; Chien, W.-M.; Wang, J. High-throughput thermodynamic computation and experimental study of solid-state phase transitions in organic multicomponent orientationally disordered phase change materials for thermal energy storage. *Calphad* **2018**, *64*, 66–77. [CrossRef]
32. Luo, A.A. Material design and development: From classical thermodynamics to CALPHAD and ICME approaches. *Calphad* **2015**, *50*, 6–22. [CrossRef]
33. Shi, R.; Luo, A.A. Applications of CALPHAD modeling and databases in advanced lightweight metallic materials. *Calphad* **2018**, *62*, 1–17. [CrossRef]
34. Shi, R.; Miao, J.; Avey, T.; Luo, A.A. A new magnesium sheet alloy with high tensile properties and room-temperature forma-bility. *Sci.Rep.* **2020**, *10*, 10044. [CrossRef] [PubMed]
35. Shi, R.; Zhu, Z.; Luo, A.A. Assessing phase equilibria and atomic mobility of intermetallic compounds in aluminum-magnesium alloy system. *J. Alloys Compd.* **2020**, *825*, 153962. [CrossRef]
36. Shi, R.; Meier, J.M.; Luo, A.A. Controlling Particle/Metal Interactions in Metal Matrix Composites during Solidification: The Role of Melt Viscosity and Cooling Rate. *Met. Mater. Trans. A* **2019**, *50*, 3736–3747. [CrossRef]
37. Shi, R.; Avey, T.; Luo, A.A. A CALPHAD (CALculation of PHAse Diagrams)-based viscosity model for Al-Ni-Fe-Co melt system. *J. Mol. Liq.* **2019**, *291*, 111271. [CrossRef]
38. Shi, R. Nonisothermal dissolution kinetics on Mg17Al12 intermetallic in Mg-Al alloys. *J. Magnes. Alloy.* **2021**, *10*, 2421–2432. [CrossRef]
39. National Research Council, Division on Engineering and Physical Sciences, National Materials Advisory Board, Committee on Integrated Computational Materials Engineering. *Integrated Computational Materials Engineering: A Transformational Discipline for Improved Competitiveness and National Security*; The National Academies Press: Washington, DC, USA, 2008.
40. Toyao, T.; Maeno, Z.; Takakusagi, S.; Kamachi, T.; Takigawa, I.; Shimizu, K.-I. Machine Learning for Catalysis Informatics: Recent Applications and Prospects. *ACS Catal.* **2019**, *10*, 2260–2297. [CrossRef]
41. Liu, Y.; Wang, L.; Zhang, H.; Zhu, G.; Wang, J.; Zhang, Y.; Zeng, X. Accelerated Development of High-Strength Magnesium Alloys by Machine Learning. *Met. Mater. Trans. A* **2021**, *52*, 943–954. [CrossRef]
42. Chen, Y.; Tian, Y.; Zhou, Y.; Fang, D.; Ding, X.; Sun, J.; Xue, D. Machine learning assisted multi-objective optimization for materials processing parameters: A case study in Mg alloy. *J. Alloys Compd.* **2020**, *844*, 156159. [CrossRef]
43. Mi, X.; Tian, L.; Tang, A.; Kang, J.; Peng, P.; She, J.; Wang, H.; Chen, X.; Pan, F. A reverse design model for high-performance and low-cost magnesium alloys by machine learning. *Comput. Mater. Sci.* **2021**, *201*, 110881. [CrossRef]
44. Wang, M.; Yu, H.; Chen, Y.; Huang, M. Machine learning assisted screening of non-rare-earth elements for Mg alloys with low stacking fault energy. *Comput. Mater. Sci.* **2021**, *196*, 110544. [CrossRef]
45. Qiao, L.; Lai, Z.; Liu, Y.; Bao, A.; Zhu, J. Modelling and Prediction of Hardness in Multi-Component Alloys: A Combined Machine Learning, First Principles and Experimental Study. *J. Alloys Compd.* **2021**, *853*, 156959. [CrossRef]
46. Gui, Y.; Li, Q.; Zhu, K.; Xue, Y. A combined machine learning and EBSD approach for the prediction of {Gui, #2} twin nucleation in an Mg-RE alloy. *Mater. Today Commun.* **2021**, *27*, 102282.
47. Messina, J.; Luo, R.; Xu, K.; Lu, G.; Deng, H.; Tschopp, M.A.; Gao, F. Machine learning to predict aluminum segregation to magnesium grain boundaries. *Scr. Mater.* **2021**, *204*, 114150. [CrossRef]
48. Jung, J.; Yoon, J.I.; Park, H.K.; Kim, J.Y.; Kim, H.S. An efficient machine learning approach to establish structure-property linkages. *Comput. Mater. Sci.* **2018**, *156*, 17–25. [CrossRef]
49. Ortego, P.; Diez-Olivan, A.; Del Ser, J.; Veiga, F.; Penalva, M.; Sierra, B. Evolutionary LSTM-FCN networks for pattern classification in industrial processes. *Swarm Evol. Comput.* **2020**, *54*, 100650. [CrossRef]
50. Mirandola, I.; Berti, G.; Caracciolo, R.; Lee, S.; Kim, N.; Quagliato, L. Machine Learning-Based Models for the Estimation of the Energy Consumption in Metal Forming Processes. *Metals* **2021**, *11*, 833. [CrossRef]
51. Palmieri, M.; Lorusso, V.; Tricarico, L. Robust Optimization and Kriging Metamodeling of Deep-Drawing Process to Obtain a Regulation Curve of Blank Holder Force. *Metals* **2021**, *11*, 319. [CrossRef]

52. Wang, D.; Xu, Y.; Duan, B.; Wang, Y.; Song, M.; Yu, H.; Liu, H. Intelligent Recognition Model of Hot Rolling Strip Edge Defects Based on Deep Learning. *Metals* **2021**, *11*, 223. [CrossRef]
53. Wu, Y.; Yan, Y.; Lv, Z. Novel Prediction Model for Steel Mechanical Properties with MSVR Based on MIC and Complex Network Clustering. *Metals* **2021**, *11*, 747. [CrossRef]
54. Lundberg, S.; Lee, S.I. A Unified Approach to Interpreting Model Predictions. *Part Adv. Neural Inf. Process. Syst.* **2017**, *30*. [CrossRef]
55. Chen, H.; Tang, J.; Gong, W.; Gao, Y.; Tian, F.; Chen, L. Effects of annealing treatment on the microstructure and corrosion behavior of hot rolled AZ31 Mg alloy. *J. Mater. Res. Technol.* **2021**, *15*, 4800–4812. [CrossRef]
56. Mohseni, M.; Eivani, A.; Vafaeenezhad, H.; Jafarian, H.; Salehi, M.; Zhou, J. An experimental and theoretical investigation of the effect of second-phase particles on grain growth during the annealing of hot-rolled AZ61 magnesium alloy. *J. Mater. Res. Technol.* **2021**, *15*, 3585–3597. [CrossRef]
57. Atwell, D.; Barnett, M.; Hutchinson, W. The effect of initial grain size and temperature on the tensile properties of magnesium alloy AZ31 sheet. *Mater. Sci. Eng. A* **2012**, *549*, 1–6. [CrossRef]
58. Bian, M.Z.; Sasaki, T.T.; Nakata, T.; Yoshida, Y.; Kawabe, N.; Kamado, S.; Hono, K. Bake-hardenable Mg–Al–Zn–Mn–Ca sheet alloy processed by twin-roll casting. *Acta Mater.* **2018**, *158*, 278–288. [CrossRef]
59. Lee, J.-Y.; Yun, Y.-S.; Suh, B.-C.; Kim, N.-J.; Kim, W.-T.; Kim, D.-H. Comparison of static recrystallization behavior in hot rolled Mg–3Al–1Zn and Mg–3Zn–0.5Ca sheets. *J. Alloys Compd.* **2014**, *589*, 240–246. [CrossRef]
60. Zhao, H.; Hua, Y.; Dong, X.; Xing, H.; Lu, Y. Influence of trace Ca addition on texture and stretch formability of AM50 magnesium alloy sheet. *Trans. Nonferrous Met. Soc. China* **2020**, *30*, 647–656. [CrossRef]
61. Nakata, T.; Xu, C.; Kaibe, K.; Yoshida, Y.; Yoshida, K.; Kamado, S. Improvement of strength and ductility synergy in a room-temperature stretch-formable Mg-Al-Mn alloy sheet by twin-roll casting and low-temperature annealing. *J. Alloys Compd.* **2022**, *10*, 1066–1074. [CrossRef]
62. Park, S.J.; Jung, H.C.; Shin, K.S. Analysis of the solidification and deformation behaviors of twin roll cast Mg-6Al-X alloys. *Met. Mater. Int.* **2016**, *22*, 1055–1064. [CrossRef]
63. He, J.; Jiang, B.; Yu, X.; Xu, J.; Jiang, Z.; Liu, B.; Pan, F. Strain path dependence of texture and property evolutions on rolled Mg-Li-Al-Zn alloy possessed of an asymmetric texture. *J. Alloys Compd.* **2017**, *698*, 771–785. [CrossRef]
64. Nakata, T.; Xu, C.; Binti Osman, N.; Geng, L.; Kamado, S. Development of corrosion-resistant Mg-Al-Ca-Mn-Zn alloy sheet with good tensile properties and stretch formability. *J. Alloys Compd.* **2022**, *910*, 164752. [CrossRef]
65. Li, Z.; Sasaki, T.T.; Bian, M.Z.; Nakata, T.; Yoshida, Y.; Kawabe, N.; Kamado, S.; Hono, K. Role of Zn on the room temperature formability and strength in Mg–Al–Ca–Mn sheet alloys. *J. Alloys Compd.* **2020**, *847*, 156347. [CrossRef]
66. Huang, X.; Bian, M.; Nakatsugawa, I.; Chino, Y.; Sato, M.; Yamazaki, K.; Kido, F.; Ueda, H.; Inoue, M. Simultaneously achieving excellent mechanical properties and high thermal conductivity in a high Mn-containing Mg-Zn-Ca-Al-Mn sheet alloy. *J. Alloys Compd.* **2021**, *887*, 161394. [CrossRef]
67. Chino, Y.; Mabuchi, M. Enhanced stretch formability of Mg–Al–Zn alloy sheets rolled at high temperature (723 K). *Scr. Mater.* **2009**, *60*, 447–450. [CrossRef]
68. Matsuoka, Y.; Bian, M.; Huang, X.; Tsukada, Y.; Koyama, T.; Chino, Y. Simulation-aided analysis on mechanical properties of dilute Mg-Zn-Ca alloy sheets. *J. Alloys Compd.* **2022**, *906*, 164285. [CrossRef]
69. Nakata, T.; Hama, T.; Sugiya, K.; Kamado, S. Understanding room-temperature deformation behavior in a dilute Mg–1.52Zn–0.09Ca (mass%) alloy sheet with weak basal texture. *Mater. Sci. Eng. A* **2022**, *852*, 143638. [CrossRef]
70. Li, Z.; Sasaki, T.T.; Bian, M.Z.; Nakata, T.; Kawabe, N.; Kamado, S.; Hono, K. Correction to: Effects of Zn Additions on the Room Temperature Formability and Strength in Mg–1.2Al–0.5Ca–0.4Mn Alloy Sheets. In *Magnesium Technology 2020*; Springer: Berlin/Heidelberg, Germany, 2020. [CrossRef]
71. Huang, L. Effect of Microalloying with Ca and Ce on Microstructure and Stamping Properties of AZ31 Alloys. Master Thesis, Chongqing University, Chongqing, China, April 2018.
72. Ma, D. Investigation on the Microstructures and Mechanical Properties of Mg-xAl-1Mn (x=1, 3, 6, 9) alloy sheets. Master Thesis, Chongqing University, Chongqing, China, May 2018.
73. Park, S.J.; Jung, H.C.; Shin, K.S. Deformation behaviors of twin roll cast Mg-Zn-X-Ca alloys for enhanced room-temperature formability. *Mater. Sci. Eng. A* **2017**, *679*, 329–339. [CrossRef]
74. Yuasa, M.; Miyazawa, N.; Hayashi, M.; Mabuchi, M.; Chino, Y. Effects of group II elements on the cold stretch formability of Mg–Zn alloys. *Acta Mater.* **2015**, *83*, 294–303. [CrossRef]
75. Nakata, T.; Xu, C.; Kamado, S. Improving tensile properties of a room-temperature formable and heat-treatable Mg–6Zn-0.2Ca (wt.%) alloy sheet via micro-alloying of Al and Mn. *Mater. Sci. Eng. A* **2020**, *772*, 138690. [CrossRef]
76. Bhattacharjee, T.; Suh, B.C.; Sasaki, T.T.; Ohkubo, T.; Kim, N.J.; Hono, K. High strength and formable Mg–6.2Zn–0.5Zr–0.2Ca alloy sheet processed by twin roll casting. *Mater. Sci. Eng. A* **2014**, *609*, 154–160. [CrossRef]
77. Zhou, M.; Huang, X.; Morisada, Y.; Fujii, H.; Chino, Y. Effects of Ca and Sr additions on microstructure, mechanical properties, and ignition temperature of hot-rolled Mg–Zn alloy. *Mater. Sci. Eng. A* **2020**, *769*, 138474. [CrossRef]
78. Zhang, Y. The Study on the Mechanisms of Strengthening and Plasticizing and Orientation Behavior in Mg-Zn Magnesium Alloys. Master Thesis, Beijing University of Science and Technology, Beijing, China, July 2020.

79. Wei, X. The investigation of Microstructure and Mechanical Properties for Mg-1.5Zn-0.2Zr(Mn)-0.2Ce(Cu) Alloys. Master Thesis, Chongqing University, Chongqing, China, May 2017.
80. Wang, P. Microstructure Control and Mechanical Properties of Wrought Mg-Zn-Ca Based Alloys with High Zn Content. Ph.D. Thesis, Jilin University, Changchun, China, June 2021.
81. Wang, Z.; Huang, Y.; Srinivasan, A.; Liu, Z.; Kainer, K.U.; Hort, N. Influences of Y Additions on the Hot Tearing Susceptibility of Mg-1.5wt.%Zn Alloys. *Mater. Sci. Forum* **2013**, *765*, 306–310.
82. Luo, A.A.; Avey, T.; Miao, J.; Meier, J.M. Magnesium Alloy Development for Structural and Biomedical Applications. *Magnesium Technol. 2022* **2022**, 3–4. Available online: https://link.springer.com/chapter/10.1007/978-3-030-92533-8_1 (accessed on 1 January 2023).
83. Bian, M.; Huang, X.; Chino, Y. A combined experimental and numerical study on room temperature formable magnesium–silver–calcium alloys. *J. Alloys Compd.* **2020**, *834*, 155017. [CrossRef]
84. Bian, M.; Huang, X.; Chino, Y. Improving flame resistance and mechanical properties of magnesium–silver–calcium sheet alloys by optimization of calcium content. *J. Alloys Compd.* **2020**, *837*, 155551. [CrossRef]
85. Wu, D.; Chen, R.S.; Han, E.H. Excellent room-temperature ductility and formability of rolled Mg–Gd–Zn alloy sheets. *J. Alloys Compd.* **2011**, *509*, 2856–2863. [CrossRef]
86. Huang, X.; Suzuki, K.; Chino, Y. Static recrystallization and mechanical properties of Mg–4Y–3RE magnesium alloy sheet processed by differential speed rolling at 823K. *Mater. Sci. Eng. A* **2012**, *538*, 281–287. [CrossRef]
87. Bian, M.; Huang, X.; Chino, Y. A room temperature formable magnesium–silver–calcium sheet alloy with high ductility. *Mater. Sci. Eng. A* **2020**, *774*, 138923. [CrossRef]
88. Bian, M.; Zeng, Z.; Xu, S.; Zhu, S.; Zhu, Y.; John Davies, C.H.; Birbilis, N.; Nie, J. Improving Formability of Mg-Ca-Zr Sheet Alloy by Microalloying of Zn. *Adv. Eng. Mater.* **2016**, *18*, 1763–1769. [CrossRef]

Disclaimer/Publisher's Note: The statements, opinions and data contained in all publications are solely those of the individual author(s) and contributor(s) and not of MDPI and/or the editor(s). MDPI and/or the editor(s) disclaim responsibility for any injury to people or property resulting from any ideas, methods, instructions or products referred to in the content.